EPJ E
Soft Matter and Biological Physics
EPJ.org
your physics journal

Eur. Phys. J. E **29**, 261–274 (2009) DOI: 10.1140/epje/i2009-10488-4

Segregation by thermal diffusion in moderately dense granular mixtures

V. Garzó

EDP SCIENCES
Società Italiana di Fisica
Springer

Eur. Phys. J. E **29**, 261–274 (2009)
DOI 10.1140/epje/i2009-10488-4

THE EUROPEAN PHYSICAL JOURNAL E

Regular Article

Segregation by thermal diffusion in moderately dense granular mixtures

V. Garzó[a]

Departamento de Física, Universidad de Extremadura, E-06071 Badajoz, Spain

Received 16 February 2009 and Received in final form 22 April 2009
Published online: 10 July 2009 –

Abstract. A theory based on a solution of the inelastic Enskog equation that goes beyond the weak dissipation limit is used to determine the thermal diffusion factor of a binary granular mixture under gravity. The Enskog equation that aims to describe moderate densities neglects velocity correlations but retains spatial correlations arising from volume exclusion effects. As expected, the thermal diffusion factor provides a segregation criterion that shows the transition between the Brazil-nut effect (BNE) and the reverse Brazil-nut effect (RBNE) by varying the parameters of the system (masses, sizes, composition, density and coefficients of restitution). The form of the phase diagrams for the BNE/RBNE transition is illustrated in detail in the tracer limit case, showing that the phase diagrams depend sensitively on the value of gravity relative to the thermal gradient. Two specific situations are considered: i) absence of gravity, and ii) homogeneous temperature. In the latter case, after some approximations, our results are consistent with previous theoretical results derived from the Enskog equation. Our results also indicate that the influence of dissipation on thermal diffusion is more important in the absence of gravity than in the opposite limit. The present analysis, which is based on a preliminary short report of the author (Phys. Rev. E **78**, 020301(R) (2008)), extends previous theoretical results derived in the dilute limit case.

PACS. 05.20.Dd Kinetic theory – 45.70.Mg Granular flow: mixing, segregation and stratification – 51.10.+y Kinetic and transport theory of gases – 05.60.-k Transport processes

1 Introduction

One of the most important phenomena occurring in granular flows containing more than one species (a polydisperse system) is the segregation and mixing of dissimilar grains. This phenomenon, in which a homogeneous mixture of different species becomes spatially non-uniform by sorting themselves in terms of their masses and/or sizes, is of central interest in the field of granular matter mainly due to its industrial importance (powder metallurgy, pharmaceutical pills, glass and paint industries, ...). The resulting non-uniformity is usually an undesirable property, although there are some applications in which one wants to force species segregation (*e.g.*, the separation of mined ores). Unfortunately, in spite of its practical relevance, the physical mechanisms that govern mixing and separation processes are not well understood yet. This fact motivates the development of fundamental theories that predict accurately the bulk behavior of these systems in order to be able to control such processes.

It is well known that when a binary mixture constituted by one large ball and a number of smaller ones is subjected to vertical shaking in a container, usually the large particle (intruder) tends to climb to the top of the sample against gravity. This phenomenon is known as the Brazil-nut effect (BNE) and is an important problem worthy to study [1–4]. On the other hand, a series of experimental works [5,6] have also observed the reverse buoyancy effect, namely, under certain conditions the intruder can also sink to the bottom of the granular bed. This effect is known as the reverse Brazil-nut effect (RBNE). Several mechanisms have been proposed to explain the transition BNE/RBNE, for example, percolation [1], arching [3], convection [2,4,7], inertia [5], condensation [6], and interstitial-fluid effects [8]. Among the different competing mechanisms, thermal diffusion becomes the most relevant one at large shaking amplitude where the sample of grains resembles a granular gas. In this regime, binary collisions prevail and kinetic theory can be a quite useful tool to analyze granular systems.

Thermal diffusion (or thermophoresis) in dilute granular mixtures has been a subject of current interest in the past few years. Thus, Serero *et al.* [9] have obtained a Chapman-Enskog solution of the Boltzmann equation given in powers of both the hydrodynamic gradients (or equivalently, the Knudsen number) and the degree of dissipation $\epsilon_{ij} = 1 - \alpha_{ij}^2$ (α_{ij} being the coefficients of restitution of the mixture). Their theory has been applied to

[a] e-mail: vicenteg@unex.es

analyze the relation between thermal diffusion and segregation in granular mixtures. In particular, they predict a novel effect, namely, the fact that even when the species differ only by their respective coefficients of restitution, they segregate when subject to a temperature gradient. Nevertheless, given that their method is based on an expansion around the elastic limit, their zeroth-order solution in the corresponding perturbation theory satisfies energy equipartition. Since this assumption can only be considered as acceptable for nearly elastic systems, some efforts have been made to assess the impact of energy non-equipartition (which is a generic feature of granular mixtures) on thermal diffusion [10,11]. In particular, the thermal diffusion factor has been recently [11] evaluated for a *dilute* granular binary mixture from a solution of the inelastic Boltzmann equation that applies for arbitrary degree of dissipation and takes into account the non-equipartition of energy. Interestingly, the results show that the relative position of the large particles (particles of mass m_1) with respect to the small particles (particles of mass m_2) is determined by the sign of the control parameter $1-(m_2T_1/m_1T_2)$, where T_1 and T_2 denote the partial temperatures of both species. While in a molecular or ordinary gas mixture this sign is fixed only by the mass ratio of the particles (since $T_1 = T_2$), for a granular gas mixture it also depends on the temperature ratio because of the lack of equipartition. This segregation criterion compares well with molecular dynamics (MD) simulations [10] carried out in the tracer limit case (namely, a binary mixture where the concentration of one of the species is negligible).

In the case of dense granular mixtures, previous relevant contributions have also been reported. Thus, Jenkins and Yoon [12] have developed a hydrodynamic theory for the segregation of *elastic* particles, finding a criterion for segregation relatively close to the numerical results obtained by Hong *et al.* [6]. In the case of binary mixtures of smooth, nearly elastic spheres, two interesting works have been carried out by Arnarson and Willits [13] and Arnarson and Jenkins [14]. While thermal diffusion factor was determined with and without gravity in the first paper [13], simplified constitutive relations for the transport coefficients of mixtures constituted by quite identical particles were derived in the second one [14]. Moreover, these authors [14] also studied segregation in a steady shearing flow with gravity transverse to the flow. On the other hand, all the above works for dense gases only apply for quasielastic particles so that non-equipartition effects on segregation are not accounted for. For this reason, more recently Trujillo *et al.* [15] have derived an evolution equation for the relative velocity of the intruder by using the Enskog kinetic theory proposed by Jenkins and Mancini [16] that is restricted to *nearly* elastic particles. Interestingly, they considered the influence of the non-equipartition of granular energy on segregation through constitutive relations for the partial pressures. These quantities (which are given in terms of the partial temperatures) are determined from the same condition as the one obtained when the granular gas is heated by means of a stochastic thermostat [17,18]. Therefore, although not explicitly stated by the authors, their results are affected by the presence of the thermostat. However, in spite of the general results obtained by Trujillo *et al.* [15], their phase diagrams for the transition BNE/RBNE have been derived by assuming that the temperature is uniform in the bulk region, so that the segregation dynamics is only driven by the gravitational force. Therefore, it appears that a complete theoretical description for the dynamics of BNE/RBNE in dense gases is still lacking.

The goal of this paper is to analyze the segregation induced by an externally imposed temperature gradient in a moderately dense granular binary mixture under gravity. The segregation criterion is obtained from the thermal diffusion factor Λ, which is given in terms of the transport coefficients of the mass flux. These coefficients are determined from the extension to driven systems of a recent solution [19,20] of the inelastic Enskog equation that covers some of the aspects not taken into account in previous works for dense gases [12,15] and extends previous results derived for dilute binary mixtures [10,11] to higher densities. Specifically, i) it takes into account the non-linear dependence of the transport coefficients on dissipation so that the theory is expected to be applicable for a wide range of values of the coefficients of restitution; ii) it considers the combined effect of gravity and thermal gradients on thermal diffusion and iii) it applies for moderate densities. Consequently, the theory subsumes all previous analysis for both dense and dilute gases, which are recovered in the appropriate limits. In addition, the theoretical predictions are in qualitative agreement with some MD simulations [10,21,22] and are also consistent with previous experimental works [23]. A preliminary short report of some of the results presented here has been given in ref. [24].

As said above, our hydrodynamic theory aims to reproduce the qualitative trends observed in real experiments of granular mixtures. In order to fluidize the system, in most of the experiments energy is added to the gas by the bottom wall which vibrates in a given way. Due to this external injection of energy, the system reaches a steady state whose properties far away from the boundaries (bulk domain) are expected to be insensitive to the details of the driving forces. However, due to the mathematical complexities associated with the use of vibrating boundary conditions, here the gas will be driven (heated) by means of a stochastic external force, coupling the velocity of each particle to a white noise. The main advantage of such a driving mechanism is that it lends itself to theoretical progress. This kind of forcing, which has been shown to be relevant for some two-dimensional experimental configurations with a rough vibrating piston [25], has been used by many authors [26] in the past years to analyze different problems, such as segregation in granular mixtures [15,24]. Although the relationship of these external forces with real vibrating walls is not clear to date, some results [11,18] derived in driven steady states for the temperature ratio by using the stochastic driving method agree quite well with MD simulations [21] of shaken mixtures. This agreement suggests that this driving method can be seen as a plausible approximation for comparison with experiments. Furthermore, since we want to compare

our theoretical results with the ones derived by Trujillo *et al.* [15] for thermalized systems, it seems natural to consider the same conditions (a granular mixture heated by the stochastic thermostat) as those assumed in ref. [15]. This is an another additional reason to consider a driven granular mixture instead of an unforced system.

The plan of the paper is as follows. First, the thermal diffusion factor Λ is defined and evaluated in sect. 2 by using a hydrodynamic description. This factor provides a convenient measure of the separation or segregation of species generated by a thermal gradient in a multicomponent system. Once Λ is expressed in terms of the pressure and the transport coefficients associated with the mass flux, these coefficients are explicitly determined by solving the Enskog kinetic equation by means of the Chapman-Enskog method. Some technical details of the extension of this method to driven systems are given in appendix A. The knowledge of the transport coefficients allows us to get Λ as a function of the parameter space of the problem, namely, the mass and diameter ratios, the composition, the three independent coefficients of restitution of the binary mixture and the solid volume fraction. In sect. 4, the form of the phase diagrams BNE/RBNE is widely investigated in the tracer limit case by varying the different parameters of the system. Moreover, a close comparison with the theoretical results [12,15] derived for thermalized (driven) dense gases is also carried out, showing that even in this limit the segregation criterion derived in this paper is more general than the one previously obtained since it covers the complete range of the parameter space of the system. The paper is closed in sect. 5 with a brief discussion of the results obtained in this paper.

2 Hydrodynamic description for segregation by thermal diffusion

We consider a binary mixture of inelastic hard disks ($d = 2$) or spheres ($d = 3$) of masses m_i and diameters σ_i ($i = 1, 2$). Without loss of generality, we assume that $\sigma_1 > \sigma_2$. The inelasticity of collisions among all pairs is characterized by three independent constant coefficients of restitution α_{11}, α_{22}, and $\alpha_{12} = \alpha_{21}$. The mixture is in presence of the gravitational field $\mathbf{g} = -g\hat{\mathbf{e}}_z$, where g is a positive constant and $\hat{\mathbf{e}}_z$ is the unit vector in the positive direction of the z axis. In the hydrodynamic description, it is assumed that the state of the mixture is characterized by the local number densities $n_i(\mathbf{r}, t)$, flow velocity $\mathbf{U}(\mathbf{r}, t)$, and temperature $T(\mathbf{r}, t)$. The time evolution of these fields is given by the balance hydrodynamic equations

$$D_t n_i + n_i \nabla \cdot \mathbf{U} + \frac{\nabla \cdot \mathbf{j}_i}{m_i} = 0, \tag{1}$$

$$D_t \mathbf{U} + \rho^{-1} \nabla \cdot \mathsf{P} = \mathbf{g}, \tag{2}$$

$$D_t T - \frac{T}{n} \sum_{i=1}^{2} \frac{\nabla \cdot \mathbf{j}_i}{m_i} + \frac{2}{dn} (\nabla \cdot \mathbf{q} + \mathsf{P} : \nabla \mathbf{U}) = -\zeta T, \tag{3}$$

where $D_t = \partial_t + \mathbf{U} \cdot \nabla$ is the material derivative, ρ is the total mass density and $n = n_1 + n_2$. In the above equations, $\mathbf{j}_i$ is the mass flux of species i, P is the pressure tensor, $\mathbf{q}$ is the heat flux, and ζ is the cooling rate associated with the energy dissipation in collisions.

In this paper, we are interested in analyzing segregation by thermal diffusion in a binary mixture [27]. Thermal diffusion is caused by the relative motion of the components of a mixture due to the presence of a thermal gradient. As a consequence of this motion, a steady state is reached in which the separating effect arising from the thermal diffusion is balanced by the remixing effect of ordinary diffusion [27]. From an experimental point of view, the amount of segregation parallel to the thermal gradient can be characterized by the thermal diffusion factor Λ. Phenomenologically, it is defined at the steady state in the absence of convection (zero flow velocity) through the relation

$$-\Lambda \frac{\partial \ln T}{\partial z} = \frac{\partial}{\partial z} \ln \left(\frac{n_1}{n_2} \right), \tag{4}$$

where gradients only along the vertical direction (z axis) have been assumed for simplicity. Let us assume that gravity and thermal gradient point in parallel directions (*i.e.*, the bottom plate is hotter than the top plate, $\partial_z \ln T < 0$). Thus, when $\Lambda > 0$, the larger particles 1 tend to rise with respect to the smaller particles 2 (*i.e.*, $\partial_z \ln(n_1/n_2) > 0$) while, when $\Lambda < 0$, the larger particles fall with respect to the smaller particles (*i.e.*, $\partial_z \ln(n_1/n_2) < 0$). The former situation is referred to as the Brazil-nut effect (BNE) while the latter is called the reverse Brazil-nut effect (RBNE).

As said before, we consider an inhomogeneous nonconvecting steady state with only gradients in the z direction. Since $\mathbf{U} = \mathbf{0}$, then the mass flux $\mathbf{j}_1 = -\mathbf{j}_2$ vanishes in the steady state according to the balance equation (1). Moreover, clearly the pressure tensor is diagonal for this state and so, $P_{ij} = p\delta_{ij}$ where p is the hydrostatic pressure. In this case, the momentum balance equation reduces to

$$\frac{\partial p}{\partial z} = -\rho g. \tag{5}$$

As will be shown later, the spatial dependence of the pressure p is through its dependence on the number densities n_i and the temperature T. As a consequence, eq. (5) can be written more explicitly as

$$\frac{p}{T} \partial_z T + \frac{\partial p}{\partial n_1} \partial_z n_1 + \frac{\partial p}{\partial n_2} \partial_z n_2 = -\rho g, \tag{6}$$

where the partial derivatives $\partial_{n_i} p$ and $\partial_T p$ will be computed once the equation of state for the mixture is obtained. To close the problem of determining Λ one needs a constitutive equation for the mass flux. Symmetry considerations yield

$$j_{1,z} = -\frac{m_1^2}{\rho} D_{11} \frac{\partial n_1}{\partial z} - \frac{m_1 m_2}{\rho} D_{12} \frac{\partial n_2}{\partial z} - \frac{\rho}{T} D_1^T \frac{\partial T}{\partial z}, \tag{7}$$

where D_{11} is the kinetic diffusion coefficient, D_{12} is the mutual diffusion coefficient, and D_1^T is the thermal diffusion coefficient. These transport coefficients measure the contribution of each independent gradient to the mass flux

of large particles (intruders). The condition $j_{1,z}=0$ yields the relation

$$x_1\lambda_1 D_{11}^* + x_2\lambda_2 D_{12}^* = -D_1^{T*}, \tag{8}$$

where $x_i = n_i/n$ is the mole fraction of species i,

$$\lambda_i = \frac{\partial_z \ln n_i}{\partial_z \ln T}\,, \tag{9}$$

and we have introduced the reduced coefficients

$$D_{ij}^* = \frac{m_i m_j \nu_0}{\rho T} D_{ij}, \qquad D_1^{T*} = \frac{\rho\nu_0}{nT} D_1^T, \tag{10}$$

where ν_0 is an effective collision frequency (to be chosen later). Moreover, in reduced units, eq. (6) can be written as

$$x_1\beta_1\lambda_1 + x_2\beta_2\lambda_2 = -(p^* + g^*). \tag{11}$$

Here, $p^* = p/nT$, $\beta_i = T^{-1}(\partial p/\partial n_i)$, and

$$g^* = \frac{\rho g}{n\left(\frac{\partial T}{\partial z}\right)} < 0 \tag{12}$$

is a dimensionless parameter measuring the gravity relative to the thermal gradient. This quantity measures the competition between these two mechanisms (g and $\partial_z T$) on segregation.

In terms of the ratios λ_i, the thermal diffusion factor can be written as

$$\Lambda = \lambda_2 - \lambda_1, \tag{13}$$

where λ_1 and λ_2 are the solution to the set of linear equations (8) and (11). Their expressions are

$$\lambda_1 = \frac{(p^*+g^*)D_{12}^* - \beta_2 D_1^{T*}}{x_1(\beta_2 D_{11}^* - \beta_1 D_{12}^*)}\,,$$

$$\lambda_2 = \frac{\beta_1 D_1^{T*} - (p^*+g^*)D_{11}^*}{x_2(\beta_2 D_{11}^* - \beta_1 D_{12}^*)}\,. \tag{14}$$

The condition $\Lambda = 0$ (or equivalently, $\lambda_1 = \lambda_2$) provides the criterion for the BNE/RBNE transition. According to eqs. (14), and assuming that $\beta_2 D_{11}^* - \beta_1 D_{12}^* \neq 0$, the condition $\lambda_1 = \lambda_2$ implies

$$(p^*+g^*)(x_1 D_{11}^* + x_2 D_{12}^*) = (x_1\beta_1 + x_2\beta_2) D_1^{T*}. \tag{15}$$

This equation gives the line delineating the regimes between BNE and RBNE. To get the dependence of the thermal diffusion factor on the parameters of the mixture, the explicit form of the transport coefficients and the equation of state is needed. This can be achieved by solving the Enskog equation by means of the Chapman-Enskog method.

3 Enskog kinetic theory

We adopt now a kinetic theory point of view and start from the Enskog kinetic equation for the system. Thus, all the macroscopic (or hydrodynamic) properties of interest of the mixture are determined from the one-particle velocity distribution functions of each species $f_i(\mathbf{r},\mathbf{v},t)$. Since thermal diffusion is given in terms of the transport coefficients D_{11}, D_{12}, and D_1^T associated with the mass flux $\mathbf{j}_1$, our goal here is to solve the corresponding set of inelastic Enskog equations by applying the Chapman-Enskog method [28] to first order in the spatial gradients. The Enskog equation neglects velocity correlations among particles which are about to collide, but it takes into account the dominant spatial corrections to the Boltzmann equation (which only applies for dilute gases) due to excluded-volume effects. Although the first assumption (molecular chaos hypothesis) can be questionable at high densities, there is substantial evidence in the literature of the accuracy of the Enskog theory for densities outside the dilute limit (moderate densities) and values of dissipation beyond the quasielastic limit [29]. As a matter of fact, this is the only available theory at present for making explicit calculations of the transport properties of moderately dense gases.

As said in the Introduction, here the mixture is driven by a stochastic external force (thermostat) that mimics the effect of a thermal bath. This external driving method is usually employed in computer simulations [26] to compensate for cooling effects associated with the inelasticity of collisions. Under these conditions, the Enskog equation for the binary mixture reads

$$\left(\frac{\partial}{\partial t} + \mathbf{v}\cdot\nabla - \frac{1}{2}\frac{\zeta_i T_i}{m_i}\frac{\partial^2}{\partial v^2} + \mathbf{g}\cdot\frac{\partial}{\partial \mathbf{v}}\right) f_i(\mathbf{r},\mathbf{v},t) = \sum_j J_{ij}[\mathbf{v}|f_i(t),f_j(t)], \tag{16}$$

where the collision operator $J_{ij}[\mathbf{v}|f_i(t),f_j(t)]$ is

$$\begin{aligned} &J_{ij}[\mathbf{r}_1,\mathbf{v}_1|f_i(t),f_j(t)] \\ &= \sigma_{ij}^{d-1}\int d\mathbf{v}_2 \int d\widehat{\boldsymbol{\sigma}}\,\Theta(\widehat{\boldsymbol{\sigma}}\cdot\mathbf{g}_{12})(\widehat{\boldsymbol{\sigma}}\cdot\mathbf{g}_{12}) \\ &\times\left[\alpha_{ij}^{-2}\chi_{ij}(\mathbf{r}_1,\mathbf{r}_1-\boldsymbol{\sigma}_{ij})f_i(\mathbf{r}_1,\mathbf{v}_1'';t)f_j(\mathbf{r}_1-\boldsymbol{\sigma}_{ij},\mathbf{v}_2'';t)\right. \\ &\left.-\chi_{ij}(\mathbf{r}_1,\mathbf{r}_1+\boldsymbol{\sigma}_{ij})f_i(\mathbf{r}_1,\mathbf{v}_1;t)f_j(\mathbf{r}_1+\boldsymbol{\sigma}_{ij},\mathbf{v}_2;t)\right]. \end{aligned} \tag{17}$$

Here, $\boldsymbol{\sigma}_{ij} = \sigma_{ij}\widehat{\boldsymbol{\sigma}}$, $\sigma_{ij} = (\sigma_i+\sigma_j)/2$, $\widehat{\boldsymbol{\sigma}}$ is a unit vector along the centers of the two colliding spheres, $\mathbf{g}_{12} = \mathbf{v}_1 - \mathbf{v}_2$, α_{ij} ($0 \le \alpha_{ij} \le 1$) is the coefficient of restitution for collisions between particles of species i and j, and χ_{ij} is the pair correlation function at contact. The precollisional velocities are given by

$$\begin{aligned} \mathbf{v}_1'' &= \mathbf{v}_1 - \mu_{ji}\left(1+\alpha_{ij}^{-1}\right)(\widehat{\boldsymbol{\sigma}}\cdot\mathbf{g}_{12})\widehat{\boldsymbol{\sigma}}, \\ \mathbf{v}_2'' &= \mathbf{v}_2 + \mu_{ij}\left(1+\alpha_{ij}^{-1}\right)(\widehat{\boldsymbol{\sigma}}\cdot\mathbf{g}_{12})\widehat{\boldsymbol{\sigma}}, \end{aligned} \tag{18}$$

where $\mu_{ij} = m_i/(m_i+m_j)$. Upon writing eq. (16), we have assumed that each species is driven by means of a stochastic Langevin force representing Gaussian white noise [30]. This force is written as $\boldsymbol{\mathcal{F}}_i = m_i\boldsymbol{\xi}$, where the covariance of the stochastic acceleration has been chosen to be the same for both species [17,31]. In the context of the Enskog equation (16), this external force is represented by a Fokker-Planck collision operator of the form $-\frac{1}{2}(\zeta_i T_i/m_i)\partial^2/\partial v^2$,

where T_i is the temperature of species i and ζ_i is the partial cooling rate associated with T_i. Note that the covariance of the external force has been taken to achieve a constant temperature in the homogeneous state. The generalization of the force to the *inhomogeneous* case is essentially a matter of choice and here, for simplicity, we have assumed that the stochastic force has the same form as in the homogeneous case except that now ζ_i and T_i are in general functions of space and time. This simple choice has been widely used in ordinary gases to analyze non-linear transport in shearing systems [32].

The Enskog kinetic equation for (undriven) multicomponent systems has been recently solved [19,20] by means of the Chapman-Enskog method [28]. The application of this method to the driven case is easy and some technical details are given in appendix A. As for elastic collisions, the transport coefficients D_{11}, D_{12}, and D_1^T are the solutions of a set of linear integral equations, which can be approximately solved by considering the first Sonine approximation. The explicit expressions for these transport coefficients and the pressure are given by eqs. (A.20, A.21) and (A.6), respectively.

The transport coefficients and the pressure are given as functions of the temperature ratio $\gamma = T_1/T_2$. This quantity measures the departure of the system from the energy equipartition. As confirmed by computer simulations [10,21,33], experiments [34] and kinetic theory calculations [35], the partial temperatures of both species are in general different. Before considering the segregation problem, the dependence of the temperature ratio γ on the parameters of the system is worth analyzing. The condition to determine the temperature ratio in the (stochastic) driven case differs from the one derived in the undriven (free cooling) case [35]. In the first case (driven case), γ is determined from the condition [17,18]

$$\frac{\zeta_1^{(0)} T_1}{m_1} = \frac{\zeta_2^{(0)} T_2}{m_2}, \tag{19}$$

while γ is obtained by requiring the equality of the cooling rates in the free cooling case, *i.e.*,

$$\zeta_1^{(0)} = \zeta_2^{(0)}. \tag{20}$$

Here, $\zeta_i^{(0)}$ are the partial cooling rates evaluated by using the zeroth-order approximation $f_i^{(0)}$ to the velocity distribution function. Their expressions are given by eq. (A.4). It must be noted that in the case of boundary conditions corresponding to a sawtooth vibration of one wall the condition to get the temperature ratio coincides with the one derived from the stochastic thermostat [18]. Since the condition to determine the ratio T_1/T_2 is different in the driven and undriven states, it is interesting to explore the similarities and differences between the temperature ratios in both situations. Note that, according to eq. (A.4), the dependence of $\zeta_1^{(0)}$ on γ in the tracer limit ($x_1 \to 0$) is through the ratio of mean-square velocities $\Theta \equiv m_2 T_1/m_1 T_2$. In terms of the parameter Θ, the conditions (19) and (20) are cubic equations with a unique real, positive solution. In particular, the behavior of the solution in the limit $\Theta \to 0$ for undriven homogeneous states has been analyzed by Santos and Dufty [36], where a change similar to a second-order phase transition has been shown. In fig. 1, we plot Θ as a function of the dimensionless quantity $h \equiv m_2(1+\alpha_{12})/2(m_1+m_2)$ in the tracer limit for a dilute gas of hard disks ($d = 2$) with $\alpha_{22} = 0.95$ and $\sigma_1/\sigma_2 = 1$. The theoretical predictions obtained from the conditions (19) and (20) indicate that Θ is a function only of the parameter h for given values of α_{22} and σ_1/σ_2 [36]. MD simulation results obtained by Brey *et al.* [10] in an open vibrated granular gas for different values of the mass ratio have been also included. It is apparent that, for the range of values explored in fig. 1, the heating mechanism slightly affects the value of Θ since the theoretical curves obtained from the driven and undriven conditions yield quite identical results. Moreover, the agreement between theory (driven and undriven cases) and simulation data is very good, except perhaps for small values of h where the results obtained in the undriven case compare with simulation data better than those derived in the driven case. On the other hand, significant differences between the results obtained with and without a thermostat for the temperature ratio T_1/T_2 are observed in fig. 2, where T_1/T_2 is plotted *versus* the size ratio σ_1/σ_2 for binary mixtures composed of spheres of the same material (and so, the same mass density, $m_1/m_2 = /(\sigma_1/\sigma_2)^3$) and equal volumes of large and small particles (*i.e.*, $x_2 = (\sigma_1/\sigma_2)^3 x_1$). The theoretical results are compared with MD simulations of Schröter *et al.* [21] in agitated mixtures with $\alpha = 0.78$. We have considered two different values of the solid volume fraction ϕ: $\phi = 0$ (low-density regime) and $\phi = 0.2$ (moderate densities). Here, for hard spheres ($d = 3$), the solid volume

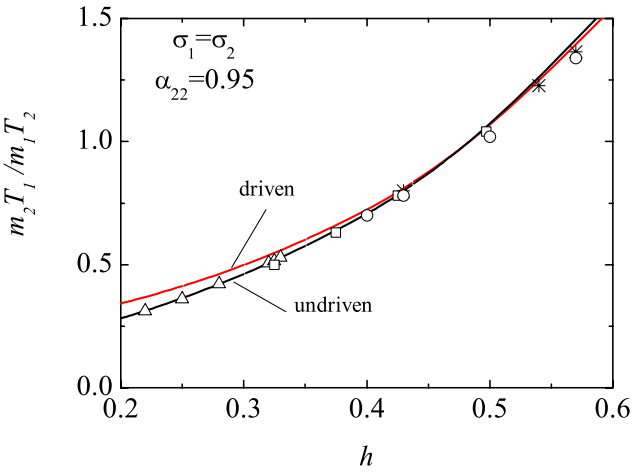

Fig. 1. (Color online) Plot of the ratio of the mean square velocities m_2T_1/m_1T_2 as a function of $h \equiv m_2(1+\alpha_{12})/2(m_1+m_2)$ for hard disks ($d = 2$), $\alpha_{22} = 0.95$, $\sigma_1/\sigma_2 = 1$ in the case of a dilute gas ($\phi = 0$) in the tracer limit ($x_1 \to 0$). The solid lines are the theoretical predictions given by eqs. (19) and (20) and the symbols are MD simulation results obtained by Brey *et al.* [10] for different values of the mass ratio: $m_1/m_2 = 2$ (triangles), 1 (squares), 0.75 (stars), and 0.5 (circles).

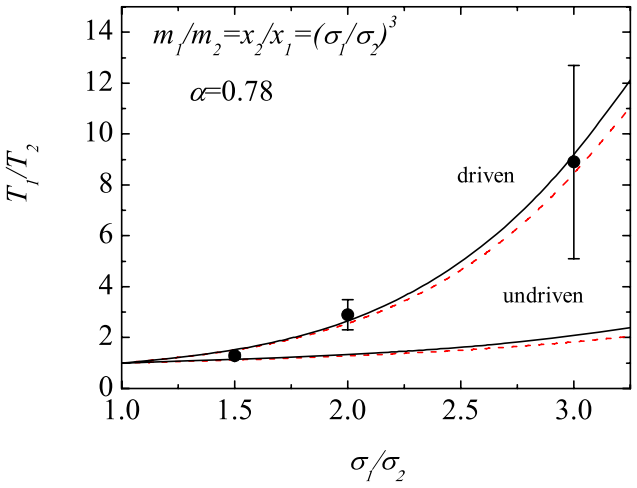

Fig. 2. (Color online) Plot of the temperature ratio T_1/T_2 as a function of the size ratio σ_1/σ_2 for $\alpha_{ij} \equiv \alpha = 0.78$ in the case of mixtures composed of spheres of the same mass density and equal total volumes of large and small particles. Two different values of the solid volume fraction have been considered: $\phi = 0$ (solid lines) and $\phi = 0.2$ (dashed lines). The points refer to MD simulations of Schröter *et al.* [21] in agitated mixtures.

fraction is defined as $\phi = (\pi/6)(n_1\sigma_1^3 + n_2\sigma_2^3)$ while for the pair correlation function evaluated at zertoh-order the following approximation has been taken [37]:

$$\chi_{ij}^{(0)} = \frac{1}{1-\phi} + \frac{3}{2}\frac{\xi}{(1-\phi)^2}\frac{\sigma_i\sigma_j}{\sigma_{ij}} + \frac{1}{2}\frac{\xi^2}{(1-\phi)^3}\left(\frac{\sigma_i\sigma_j}{\sigma_{ij}}\right)^2, \tag{21}$$

where $\xi = (\pi/6)(n_1\sigma_1^2 + n_2\sigma_2^2)$. It is evident that the disagreement found in fig. 2 illustrates the fact that the heating mechanisms affect in general non-equipartition even in the bulk of the system [38]. While a good agreement between kinetic theory and MD simulations is found when the mixture is heated by the stochastic thermostat, important discrepancies appear in the undriven case, especially as the size ratio increases. We also observe a weak influence of density on the temperature ratio. As noted in a previous work [11], the good agreement found in fig. 2 stimulates the use of this driving method for qualitative comparisons with experimental results and is one of the main reasons for which the above thermostat has been introduced in the segregation problem studied in this paper. On the other hand, given the results reported in fig. 1 in the tracer limit case for dilute gases, more simulation data are needed to make quantitative comparisons between theories based on homogeneously heated granular systems and boundary-driven problems in order to assess the reliability of the above theoretical predictions.

4 Intruder limit case: Phase diagrams for the BNE/RBNE transition

Once the form of the transport coefficients is known, the thermal diffusion factor Λ can be explicitly obtained when one substitutes eqs. (A.20, A.21) for D_1^T, D_{11}, and D_{12}, respectively, and eq. (A.6) for p into eqs. (13) and (14). This gives the dependence of Λ in terms of the parameter space of the problem. On the other hand, the explicit evaluation of the expressions for the different transport coefficients for a variety of masses, diameters, composition, dissipation and density is still intricate. In subsequent publications, we will analyze the quantitative variation of such coefficients (along with those associated with the momentum and heat fluxes) across this parameter set of the system. Here, in order to show more clearly the different competing mechanisms appearing in the segregation phenomenon, we consider the tracer limit case, namely, a binary mixture where the concentration of one of the components (the tracer or intruder) is very small compared to that of the other (solvent or excess) component. This limit case ($x_1 \to 0$) allows us to present a simplified theory where a segregation criterion can be explicitly obtained.

Under these conditions, when one considers the form of the transport coefficients (eqs. (A.25–A.27)) in the tracer limit, the criterion (15) can be written as

$$g^*(\gamma - M) + \phi\left[(\gamma - Mg^*)\frac{\partial p^*}{\partial\phi} - M\frac{p^*-1}{\phi}g^*\right] + \frac{(1+\omega)^d}{2}\frac{M}{1+M}\chi_{12}^{(0)}\phi(1+\alpha_{12})\left[(p^*+g^*)\frac{M+\gamma}{M}\Delta - \beta\right] = 0. \tag{22}$$

Here, $M = m_1/m_2$ is the mass ratio, $\omega = \sigma_1/\sigma_2$ is the diameter ratio, $\beta = p^* + \phi\partial_\phi p^*$,

$$p^* = 1 + 2^{d-2}\chi_{22}^{(0)}\phi(1+\alpha_{22}) \tag{23}$$

is the (reduced) pressure of the gas [39,40] and

$$\phi \equiv \frac{\pi^{d/2}}{2^{d-1}d\Gamma(d/2)}n_2\sigma_2^d \tag{24}$$

is the solid volume fraction. Moreover,

$$\Delta \equiv \frac{(1+\omega)^{-d}}{\chi_{12}^{(0)}T}\left(\frac{\partial\mu_1}{\partial\phi}\right)_{T,n_1}, \tag{25}$$

where μ_1 is the chemical potential of the intruder. Equation (25) contains all the information necessary to describe the segregation due to thermal (or Soret) diffusion of an intruder in a moderately dense granular fluid. The first term on the left-hand side measures essentially the influence of the non-equipartition of the granular energy on segregation. This term vanishes in the absence of the gravitational force. The second and third terms are proportional to the solid volume fraction ϕ and so, they account for the effects of density on thermal diffusion. These latter two terms vanish in the dilute limit case ($\phi \to 0$). The influence of each term on the segregation criterion (22) depends on the specific values of dissipation (which is for instance the main responsible for the energy non-equipartition), density, mechanical parameters of the system and/or (reduced) gravity.

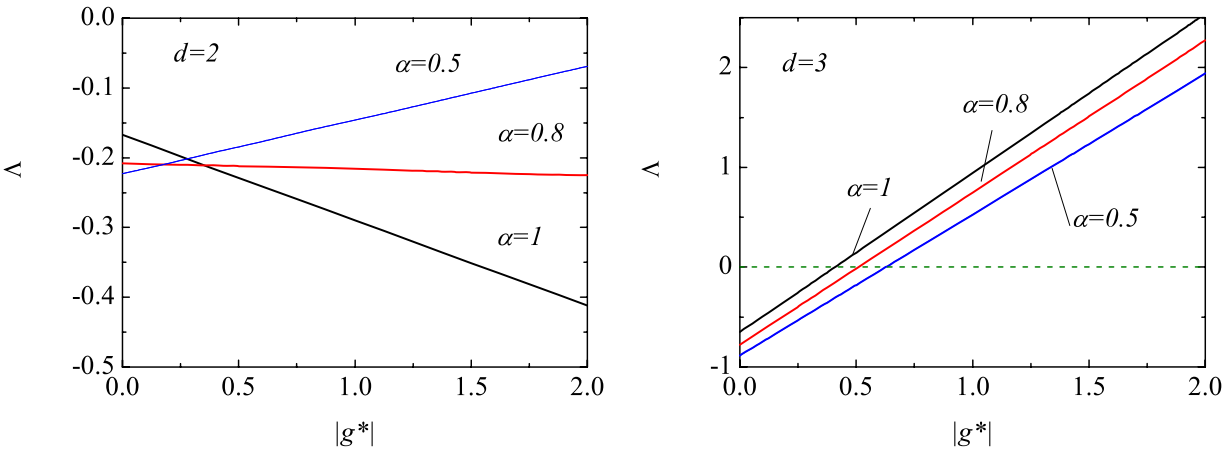

Fig. 3. (Color online) Plot of the thermal diffusion factor Λ *versus* the (reduced) gravity $|g^*|$ for $m_1/m_2 = \sigma_1/\sigma_2 = 2$, $\phi = 0.2$ and three values of the (common) coefficient of restitution $\alpha \equiv \alpha_{22} = \alpha_{12}$. The left panel is for hard disks ($d = 2$) while the right panel is for hard spheres ($d = 3$).

Before exploring the dependence of the parameter space on the form of the phase diagrams BNE/RBNE, it is instructive to consider some special limit situations. Thus, when the intruder and particles of the gas are mechanically equivalent ($m_1 = m_2$, $\sigma_1 = \sigma_2$, and $\alpha_{12} = \alpha_{22}$), then as expected the two species do not segregate. This is consistent with eq. (22) since in this limit case $D_1^{T*} = D_{11}^* + D_{12}^* = 0$ and so $\Lambda = 0$ for any value of α_{ij} and ϕ. On the other hand, in the case of a dilute gas ($\phi \to 0$), then eq. (22) yields

$$g^*(\gamma - M) = 0. \tag{26}$$

In the absence of gravity, eq. (26) holds trivially, so that the intruder does not segregate in a dilute gas when $g^* = 0$. This result is due to the failure of the first Sonine approximation to accurately describe this special situation since segregation would appear if one retained higher-order terms in the Sonine polynomial expansion [27,41]. On the other hand, when $|g^*| \neq 0$, the solution to eq. (26) is

$$\frac{T_1}{T_2} = \frac{m_1}{m_2}. \tag{27}$$

This result agrees with recent results derived from the Boltzmann equation [10,11]. Note that, due to the lack of energy equipartition, the criterion (27) is rather complicated since it involves all the parameter space. The segregation criterion (27) compares well with MD simulation results for the case of the steady state of an open vibrated granular system in the absence of macroscopic fluxes [10].

In the tracer limit, the parameter space is sixfold: the dimensionless gravity g^*, the mass ratio m_1/m_2, the size ratio σ_1/σ_2, the coefficients of restitution α_{22} and α_{12} and the solid volume fraction ϕ. In order to get the phase diagrams for the BNE/RBNE transition, one has to give the form of the pair correlation functions $\chi_{22}^{(0)}$ and $\chi_{12}^{(0)}$ and the chemical potential μ_1. In the three-dimensional case, the pair correlation functions can be easily obtained from eq. (21) by taking the limit $x_1 \to 0$, namely,

$$\chi_{22}^{(0)} = \frac{1 - \frac{1}{2}\phi}{(1-\phi)^3},$$
$$\chi_{12}^{(0)} = \frac{1}{1-\phi} + 3\frac{\omega}{1+\omega}\frac{\phi}{(1-\phi)^2} + 2\frac{\omega^2}{(1+\omega)^2}\frac{\phi^2}{(1-\phi)^3}. \tag{28}$$

The expression for the chemical potential of the intruder consistent with the approximation (28) is [42]

$$\frac{\mu_1}{T} = C_3 + \ln n_1 - \ln(1-\phi) + 3\omega\frac{\phi}{1-\phi} + 3\omega^2\left[\ln(1-\phi) + \frac{\phi(2-\phi)}{(1-\phi)^2}\right] - \omega^3\left[2\ln(1-\phi) + \frac{\phi(1-6\phi+3\phi^2)}{(1-\phi)^3}\right], \tag{29}$$

where C_3 is a constant. For hard disks ($d = 2$), $\chi_{22}^{(0)}$ and $\chi_{12}^{(0)}$ are approximately given by [16]

$$\chi_{22}^{(0)} = \frac{1 - \frac{7}{16}\phi}{(1-\phi)^2}, \quad \chi_{12}^{(0)} = \frac{1}{1-\phi} + \frac{9}{8}\frac{\omega}{1+\omega}\frac{\phi}{(1-\phi)^2}. \tag{30}$$

Now, the form of the chemical potential consistent with the above approximations is [43]

$$\frac{\mu_1}{T} = C_2 + \ln n_1 - \ln(1-\phi) + \frac{1}{4}\omega\left[\frac{9\phi}{1-\phi} + \ln(1-\phi)\right] + \frac{1}{8}\omega^2\left[\frac{\phi(7+2\phi)}{(1-\phi)^2} - \ln(1-\phi)\right], \tag{31}$$

where C_2 is a constant.

Equations (13) and (14) clearly show that Λ is a linear function of gravity g^*. This is illustrated in fig. 3 where thermal diffusion is plotted as a function of $|g^*|$ for hard disks ($d = 2$) and spheres ($d = 3$). We have considered the system $m_1/m_2 = \sigma_1/\sigma_2 = 2$, $\phi = 0.2$ and several values of

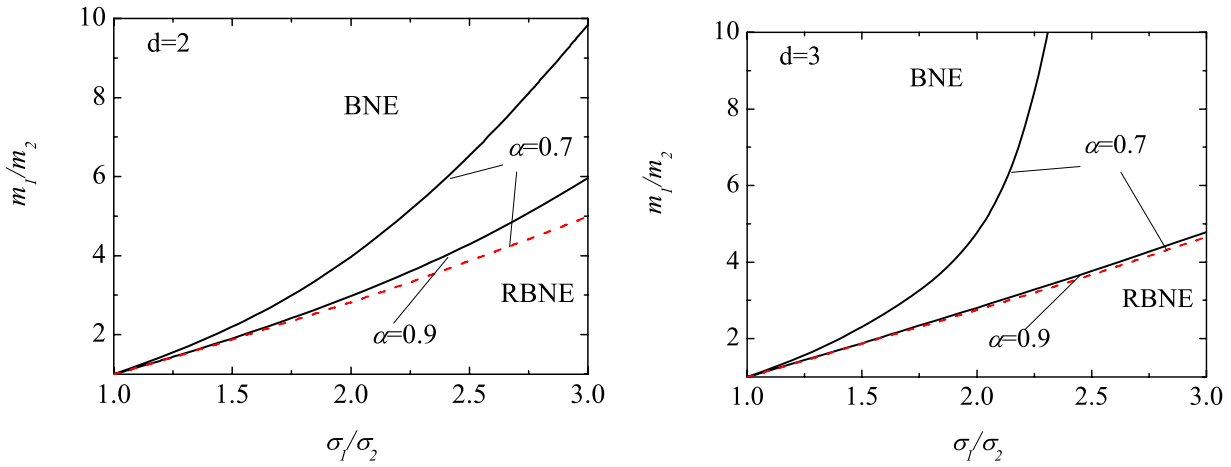

Fig. 4. (Color online) Phase diagram for BNE/RBNE for $\phi = 0.25$ in the absence of gravity ($g^* = 0$) for two values of the (common) coefficient of restitution $\alpha \equiv \alpha_{22} = \alpha_{12}$. Points above the curve correspond to $\Lambda > 0$ (BNE) while points below the curve correspond to $\Lambda < 0$ (RBNE). The dashed line is the result obtained for $\alpha = 0.7$ assuming energy equipartition ($T_1 = T_2$). The top panel is for hard disks ($d = 2$) while the bottom panel is for hard spheres ($d = 3$).

the (common) coefficient of restitution $\alpha \equiv \alpha_{22} = \alpha_{12}$. It is apparent for the case analyzed here that the RBNE is dominant for hard disks in all the range of values of gravity (except for $\alpha = 0.5$ where a change to BNE is expected for values of $|g^*|$ larger than 2) while the RBNE is only dominant at small $|g^*|$ for hard spheres. Thus, as already noted in ref. [24], for given values of m_1/m_2, σ_1/σ_2, α_{22}, α_{12} and ϕ there is a critical value $|g_c^*|$ such that a transition BNE $\Leftrightarrow$ RBNE (or RBNE $\Leftrightarrow$ BNE) is observed for $|g^*| > |g_c^*|$. We see that the value of $|g_c^*|$ increases with dissipation.

According to eq. (22), segregation is driven and sustained by both gravity and temperature gradients. The combined effect of both g and $\partial_z T$ on thermal diffusion is through the dimensionless gravity $g^* < 0$ defined by eq. (12). This parameter measures the competion between both mechanisms on segregation. Although our perturbation approach assumes that both gravity and thermal gradient are of the same order of magnitude, it is interesting for illustrative purposes to separate the influence of each one of the terms appearing in eq. (22) on segregation. Therefore, some specific cases ($g = 0$ or $\partial_z T \to 0$) will be considered in the next subsections.

4.1 Absence of gravity ($|g^*| \to 0$)

Let us study first the segregation of two species of grains in the presence of a temperature gradient, but in the absence of gravity ($g = 0$). This limit has been considered in some MD simulations (see, for example, the simulations carried out by Galvin *et al.* [22]). In this case, $|g^*| \to 0$ and eq. (22) reduces to

$$\gamma\phi\frac{\partial p^*}{\partial\phi} = \frac{(1+\omega)^d}{2}\frac{M}{1+M}\chi_{12}^{(0)}\phi(1+\alpha_{12}) \times\left[\phi\frac{\partial p^*}{\partial\phi} + p^*\left(1 - \Delta\frac{\gamma+M}{M}\right)\right]. \quad (32)$$

Of course, this equation is trivially satisfied in the case of a dilute gas ($\phi = 0$). Beyond the dilute limit, the influence of each term in (32) is still intricate. As an illustration, fig. 4 shows the phase diagram in the $\{m_1/m_2, \sigma_1/\sigma_2\}$-plane at a total volume fraction of $\phi = 0.25$ (moderately dense gas) and two different values of the (common) coefficient of restitution $\alpha_0 = \alpha$. It is apparent that, in the absence of gravity, the main effect of dissipation is to reduce the size of the BNE. This effect is more significant in the case of hard spheres than in the case of disks. We observe that in general the RBNE (intruders move towards the hot regions) is dominant for both small mass ratio and/or large size ratio. In order to assess the impact of the non-equipartition of granular energy on segregation, we have also plotted the corresponding phase diagram for $\alpha = 0.7$ but assuming that $T_1 = T_2$. The comparison between both curves clearly shows the significant influence of the temperature differences on thermal diffusion in the absence of gravity. This is consistent with the recent MD findings of Galvin *et al.* [22] where they showed that non-equipartition driving forces for segregation are comparable to other driving forces for systems displaying moderate level of non-equipartition. Figure 5 illustrates the influence of the volume fraction on the phase diagram for a three-dimensional system at moderate level of dissipation ($\alpha = 0.8$). It is apparent that the role played by the density is quite important since the range of size and mass ratios for which the RBNE exists increases with decreasing ϕ. Note that when both the mass and diameter ratios of the intruder are very large, the state of the gas could be disturbed by the presence of the intruder. In this case, the results obtained from eq. (22) could be questionable since they have been obtained by neglecting the cross-collision term in the kinetic equation for the gas particles.

4.2 Thermalized systems ($\partial_z T \to 0$)

We consider now a system in which the inhomogeneities in both the temperature and the mixture volume fraction

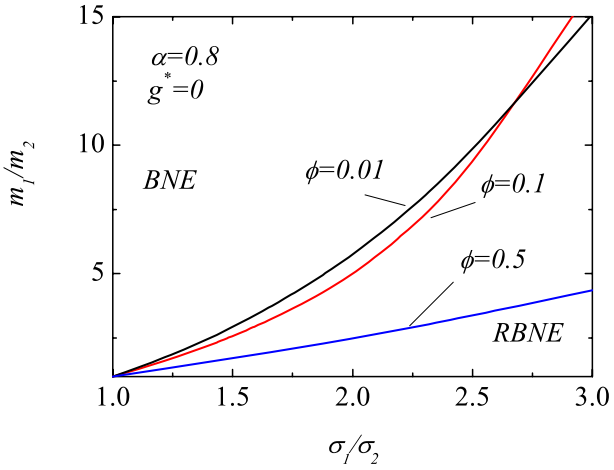

Fig. 5. (Color online) Phase diagram for BNE/RBNE for inelastic hard spheres for $\alpha \equiv \alpha_{22} = \alpha_{12} = 0.8$, $|g^*| = 0$ and three different values of the solid volume fraction ϕ.

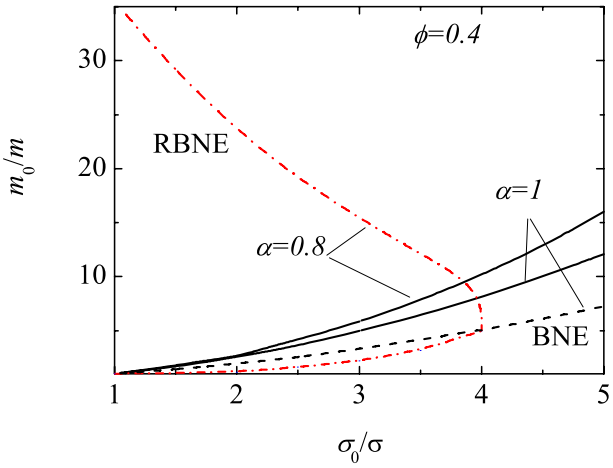

Fig. 6. (Color online) Phase diagram for BNE/RBNE for a two-dimensional system in the absence of thermal gradient ($|g^*| \to \infty$) at $\phi = 0.4$ and two values of the (common) coefficient of restitution $\alpha \equiv \alpha_{22} = \alpha_{12}$. The dashed and dashed-dotted lines refer to the results obtained by Jenkins and Yoon [12] for elastic gases ($\alpha = 1$) and by Trujillo *et al.* [15] for $\alpha = 0.8$, respectively.

are neglected ($\partial_z T \to 0$) but gravity is different from zero. In this case, the segregation dynamics of the intruders is essentially driven by the gravitational force. This situation (gravity dominates the temperature gradient) can be achieved in the shaken or sheared systems employed in numerical simulations and physical experiments [6,23,44, 45]. Under these conditions ($|g^*| \to \infty$), the criterion (22) can be written as

$$\frac{1+\frac{(1+\omega)^d}{2}\chi_{12}^{(0)}\phi(1+\alpha_{12})\frac{\gamma+M}{1+M}\frac{\Delta}{\gamma}}{1+2^{d-2}\chi_{22}^{(0)}\phi(1+\alpha_{22})\left[1+\phi\partial_\phi\ln\left(\phi\chi_{22}^{(0)}\right)\right]}\frac{T_1}{T_2}=\frac{m_1}{m_2}\,. \tag{33}$$

As said in the Introduction, previous theoretical attempts to describe this particular situation have been made independently by Jenkins and Yoon [12] for elastic systems and by Trujillo *et al.* [15] for inelastic systems. Both descriptions are based on a kinetic theory [16] that is restricted to the quasielastic limit ($\alpha_{ij} \to 1$), although Trujillo *et al.* [15] take into account the effect of non-equipartition of energy on segregation. Their segregation criterion differs from eq. (33) and is given by [15]

$$\frac{1+\frac{(1+\omega)^d}{2}\chi_{12}^{(0)}\phi}{1+2^{d-1}\chi_{22}^{(0)}\phi}\frac{T_1}{T_2}=\frac{m_1}{m_2}\,, \tag{34}$$

which is consistent with the one derived by Jenkins and Yoon [12] when $\alpha_{22} = \alpha_{12} = 1$. The discrepancies between eqs. (33) and (34) can be attributed to the simplicity of the kinetic theory used for deriving the latter criterion. In particular, it is easy to see that eq. (33) reduces to eq. (34) when one i) neglects the dependence on inelasticity and assumes equipartition in certain terms, ii) takes the approximation $\Delta = 1$ (which only applies for a dilute gas of mechanically equivalent particles), and iii) neglects high density corrections (last term in the denominator of (33)). Therefore, in relation to the above previous results, we can conclude that the criterion (33) is more general than the one derived by Trujillo *et al.* [15], since our results are not restricted to nearly elastic gases.

A typical phase diagram for thermalized systems delineating the regimes between BNE and RBNE is plotted in fig. 6 for the two-dimensional case. (The qualitative features of the corresponding phase diagram for the three-dimensional case are similar.) Comparison between the left panel of fig. 4 (hard disks) and fig. 6 clearly shows that the presence of gravity changes dramatically the form of the phase diagram. In particular, the main effect of inelasticity is to reduce the size of the RBNE region, which is consistent with experiments [23]. Moreover, we also observe that the RBNE regime appears essentially now for both large mass ratio and/or small diameter ratio. On the other hand, the predictions of Trujillo *et al.* [15] for $\alpha = 0.8$ disagree with our results even at a qualitative level since they find that the mass ratio is a two-valued function of the size ratio in the phase diagram. In fact, according to the results of Trujillo *et al.* [15], the effect of dissipation is to introduce a threshold size ratio above which there is no RBNE. We also observe that our results differ from those obtained by Jenkins and Yoon [12] for elastic gases, especially for large size ratios. Our results also indicate (not shown in fig. 6) that non-equipartition has a weaker influence on segregation for thermalized systems than in the opposite limit (absence of gravity). This behavior qualitatively agrees with the experiments carried out by Schröter *et al.* [21] for vibrated mixtures as well as with some recent theoretical results of Yoon and Jenkins [46] since both works find that segregation (when is only driven by gravity) is not significantly influenced by the difference between the temperatures of the two species.

4.3 General case

Finally, we consider the effect of density for finite values of the reduced gravity $|g^*|$. Figure 7 shows a phase

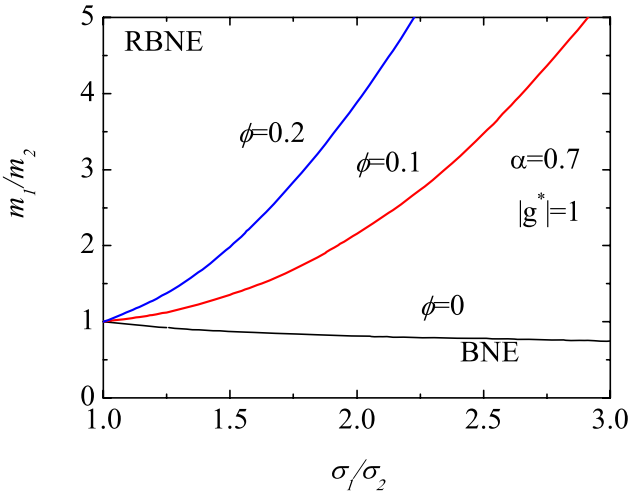

Fig. 7. (Color online) Phase diagram for BNE/RBNE for inelastic hard spheres for $\alpha \equiv \alpha_{22} = \alpha_{12} = 0.7$, $|g^*| = 1$ and three different values of the solid volume fraction ϕ.

diagram when $|g^*| = 1$ (gravity comparable to the thermal gradient) for different values of the volume fraction. We have considered inelastic hard spheres ($d = 3$) with $\alpha_{22} = \alpha_{12} = 0.7$. In contrast to fig. 5, we observe that the RBNE regime appears essentially now for both large mass ratio and/or small size ratio. Regarding the influence of density on the form of the phase diagram, it is apparent that the regime of the RBNE decreases significantly with increasing ϕ. Following Trujillo *et al.* [15], in the fluidized regime the effect of shaking strength of vibration on the phase diagram for BNE/RBNE can be tied to the effect of varying the solid volume fraction ϕ. According to this argument, fig. 7 shows that the possibility of RBNE increases with increasing shaking strength (or decreasing density). The experimental findings of Breu *et al.* [23] show similar trends with increasing shaking strength, which is consistent with our results.

5 Conclusions

The problem of segregation by thermal diffusion in a binary granular mixture has been addressed in this paper. Thermal diffusion is the relevant segregation mechanism in agitated granular mixtures at large shaking amplitude. In this situation, the thermal diffusion factor Λ (defined by eq. (4)) characterizes the amount of segregation parallel to the thermal gradient [27]. Here, the factor Λ has been obtained in a non-convecting steady state with gradients only along the vertical direction (parallel to gravity). Two complementary approaches have been followed to evaluate the thermal diffusion. First, by using a hydrodynamic description Λ has been expressed in terms of the pressure and the transport coefficients associated with the mass flux. Then, the above quantities have been explicitly determined by solving the inelastic Enskog equation by means of the Chapman-Enskog method [28]. This allow us to determine Λ as a function of the mass and size ratios, the composition, the coefficients of restitution, the solid volume fraction and the reduced gravity $g^* = \rho g/n\partial_z T < 0$. Once the explicit form of Λ is known, the condition $\Lambda = 0$ provides the segregation criterion for the transition BNE $\Leftrightarrow$ RBNE. This criterion is given by eq. (15) in terms of the transport coefficients whose expressions are given by eqs. (A.20, A.21).

One of the main objectives of this paper has been to extend the analysis made in ref. [11] to higher densities by considering the revised Enskog kinetic theory. By extending the Boltzmann analysis to high densities, comparisons with MD simulations become practical and allow one to quantitatively test the use of a hydrodynamic description for segregation in granular vibrated mixtures. On the other hand, given that the Enskog equation still assumes uncorrelated particle velocities (molecular chaos hypothesis), it is expected that our results apply for moderate densities (solid volume fractions typically smaller than or equal to 0.2). Furthermore, the segregation criterion derived in this paper has been obtained by using the first Sonine approximation for the transport coefficients whose accuracy can be questionable for strong values of dissipation and/or disparate values of the mass and size ratios [41]. This is one of the restrictions of the results offered here. Another ingredient in our theory is the use of a driving stochastic thermostat instead of using vibrating boundary conditions to fluidize the system. Although previous experiments in agitated mixtures [34] have shown a less significant dependence of the temperature ratio T_1/T_2 on inelasticity than the one obtained in driven steady states [18], it must be remarked that the results derived here and in ref. [11] for the temperature ratio from this stochastic driving method compare quite well with MD simulations of agitated mixtures [21]. As said in the Introduction, this agreement could justify the use of this kind of thermostat as a first approximation to make comparisons with experiments of vibrated mixtures.

Some previous theoretical efforts [12,13,15] on the same topic for dense granular mixtures have been made. However, they have been based on kinetic theories which are valid for nearly elastic particles [13] and have considered situations where the temperature has been assumed to be homogeneous (and so, the effects of the temperature gradient on segregation have been neglected) [15]. The present study goes beyond the weak dissipation limit and takes into account the influence of both thermal gradient and gravity through the reduced gravity g^*. Moreover, previous results [10,11] obtained in the dilute regime limit are recovered at zero density ($\phi \to 0$).

In order to illustrate the form of the phase diagrams BNE/RBNE in the mass and size ratio plane, the tracer or intruder limit case has been considered. This limit simplifies the evaluation of the transport coefficients (since for instance, the temperature ratio is independent of composition and so, $\partial\gamma/\partial n_i = 0$) and in addition, it allows us to clearly present the different competing mechanisms appearing in the segregation phenomena. Under these conditions, the segregation criterion for the transition BNE $\Leftrightarrow$ RBNE is given by eq. (22). This is one of the most important results of the paper. Two specific

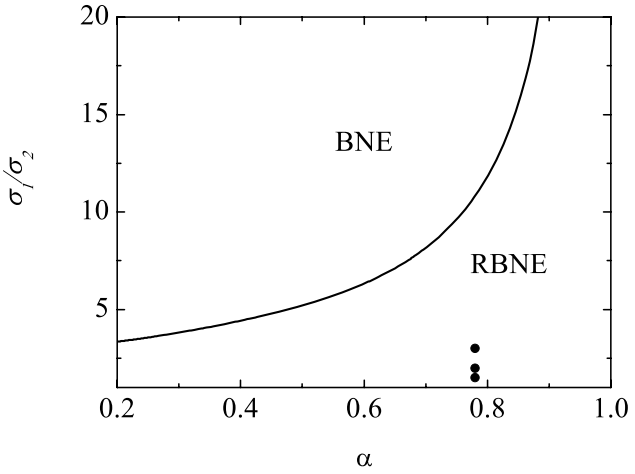

Fig. 8. Phase diagram for BNE/RBNE for a dilute binary mixture composed of spheres of the same mass density and equal total volumes of large and small particles. The data points represent the simulation results of Schröter *et al.* [21] for $\alpha = 0.78$ when convection is suppressed.

situations have been mainly studied: $g^* = 0$ (absence of gravity) and $|g^*| \to \infty$ (homogeneous temperature). The first case has been considered in recent MD simulations [22] while the second case has been widely studied by using kinetic theory [12,15], computer simulations [21] and experiments [23]. Our results show that the influence of dissipation on thermal diffusion is more important when the thermal gradient dominates over gravity ($g^* = 0$) than in the opposite limit ($|g^*| \to \infty$). This weak influence on dissipation in the latter case contrasts with the results of Trujillo *et al.* [15] since they found that the main effect of inelasticity is to introduce a threshold size ratio above which there is no RBNE (see fig. 6). We attribute this discrepancy with ref. [15] to the use of some (uncontrolled) approximations in the expressions of the partial pressures and the transport coefficients. Regarding the role played by the non-equipartition of granular energy (pseudo-thermal buoyancy force) in the segregation process, our results indicate (see fig. 4) that, while the temperature difference has an important influence on thermal diffusion in the absence of gravity, it has a weaker effect on segregation when gravity dominates over thermal gradient. These conclusions agree qualitatively well with recent MD simulations [22] and with some experiments carried out by Schröter *et al.* [21] in vibrated mixtures.

Although the theory reported in this paper is consistent with previous numerical and experimental results, a more quantitative comparison with the latter is desirable. To make some contact with experiments of size segregation driven by thermal diffusion, let us consider again the results obtained by Schröter *et al.* [21] for spheres made of particles with the same mass density and equal total volumes of large and small particles. Specifically, we consider the simulation data reported in fig. 11 of ref. [21] when the convection has been suppressed. Here, for the sake of simplicity, we consider the segregation criterion given by eq. (15) for a dilute binary mixture ($\phi = 0$) with $m_1/m_2 = x_2/x_1 = (\sigma_1/\sigma_2)^3$ and a common coefficient of restitution ($\alpha_{ij} \equiv \alpha$). Figure 8 shows the phase diagram for this kind of systems where the data points represent the MD results for $\alpha = 0.78$ (the experimental value of the coefficient of restitution considered). It is apparent that, although the RBNE is dominant at small diameter ratios, there is a crossover to BNE at sufficiently large diameter ratios. As noted in ref. [11], the form of this phase diagram agrees qualitatively with the findings of ref. [21] for this type of conditions since they do not observe a change back to BNE for diameter ratios up to $\sigma_1/\sigma_2 = 3$ (see red squares in fig. 11 of [21]). Moreover, although the range of values for the size ratio considered in MD simulations is smaller than the one studied here theoretically, one could roughly obtain the transition value of the diameter ratio by extrapolating their simulation data. In this case, an extrapolation from their simulation data at the diameter ratios of 2 and 3 shows that the transition from RBNE to BNE might be around $\sigma_1/\sigma_2 = 10$. This value quantitatively agrees with our theoretical curve at $\alpha = 0.78$. We expect that this agreement is also kept for experiments carried at higher densities. In this context, it is hoped that this paper stimulates the performance of such simulations.

Finally, it must be noted that, although the results derived in this paper for thermal diffusion hold for general binary mixtures (with arbitrary values of composition x_1), only the limit of a single intruder ($x_1 \to 0$) has been widely investigated. This limit precludes the possibility of analyzing the influence of composition on the thermal diffusion factor Λ, where previous results for dilute gases [11] have shown that the effect of x_1 on Λ can be significant in many situations. The study on the dependence of thermal diffusion on composition is an interesting open problem. I plan to carry out such work in the near future.

I am grateful to María José Ruiz-Montero for providing me the simulation data for fig. 1. This work has been supported by the Ministerio de Educación y Ciencia (Spain) through grant No. FIS2007-60977, partially financed by FEDER funds and by the Junta de Extremadura (Spain) through Grant No. GRU09038.

Appendix A. Chapman-Enskog solution in the driven case

In this appendix we solve the set of Enskog equations (16) to first order in the spatial gradients by means of the Chapman-Enskog method [28]. From this solution, we determine then the transport coefficients D_{11}, D_{12} and D_1^T associated with the mass flux.

The zeroth-order distribution function $f_i^{(0)}$ obeys the Enskog equation

$$-\frac{\zeta_i^{(0)} T_i}{2m_i}\frac{\partial^2}{\partial V^2} f_i^{(0)} = \sum_j J_{ij}^{(0)}\left[f_i^{(0)}, f_j^{(0)}\right], \qquad \text{(A.1)}$$

where

$$J_{ij}^{(0)}\left[f_i^{(0)},f_j^{(0)}\right]=\chi_{ij}^{(0)}\sigma_{ij}^{d-1}\int d\mathbf{v}_2\int d\widehat{\boldsymbol{\sigma}}\Theta(\widehat{\boldsymbol{\sigma}}\cdot\mathbf{g}_{12})\times(\widehat{\boldsymbol{\sigma}}\cdot\mathbf{g}_{12})\left[\alpha_{ij}^{-2}f_i^{(0)}(\mathbf{v}_1'')f_j(\mathbf{v}_2'')-f_i^{(0)}(\mathbf{v}_1)f_j^{(0)}(\mathbf{v}_2)\right]. \tag{A.2}$$

Upon writing eq. (A.1) use has been made of the fact that $\partial_t^{(0)}T=0$ at this order in the driven case. Moreover, $\zeta_i^{(0)}$ refers to the partial cooling rate evaluated by using the zeroth-order velocity distribution function $f_i^{(0)}$. Since the latter is not exactly known, one has to expand $f_i^{(0)}$ in Sonine polynomials. A good approximation for it (at least for not very strong inelasticity) is given by the Gaussian distribution

$$f_i^{(0)}(V)\to f_{i,M}(V)=n_i\left(\frac{m_i}{2\pi T_i}\right)^{d/2}e^{-m_iV^2/2T_i}, \tag{A.3}$$

where $\mathbf{V}=\mathbf{v}-\mathbf{U}$. Employing it, one gets

$$\zeta_i^{(0)}=\frac{4\pi^{(d-1)/2}}{d\Gamma\left(\frac{d}{2}\right)}v_0\sum_{j=1}^{2}n_j\mu_{ji}\sigma_{ij}^{d-1}\chi_{ij}^{(0)}\left(\frac{\theta_i+\theta_j}{\theta_i\theta_j}\right)^{1/2}\times(1+\alpha_{ij})\left[1-\frac{\mu_{ji}}{2}(1+\alpha_{ij})\frac{\theta_i+\theta_j}{\theta_j}\right], \tag{A.4}$$

where $v_0=\sqrt{2T(m_1+m_2)/m_1m_2}$ is a thermal velocity defined in terms of the global temperature T of the mixture and

$$\theta_i=\frac{m_i}{\gamma_i}\sum_{j=1}^{2}m_j^{-1}. \tag{A.5}$$

The pressure p is given by [19]

$$p=nT\left[1+\frac{\pi^{d/2}}{d\Gamma\left(\frac{d}{2}\right)}\sum_{i=1}^{2}\sum_{j=1}^{2}\mu_{ji}n\sigma_{ij}^{d}\chi_{ij}^{(0)}x_ix_j(1+\alpha_{ij})\gamma_i\right], \tag{A.6}$$

where

$$\gamma_1=\frac{\gamma}{1+x_1(\gamma-1)},\quad \gamma_2=\frac{1}{1+x_1(\gamma-1)}, \tag{A.7}$$

and $\gamma=T_1/T_2$ is the temperature ratio.

The determination of the first-order distribution $f_i^{(1)}$ follows similar mathematical steps as those made in the undriven case for polydisperse systems [19]. Here, we only display some partial results. The distribution $f_i^{(1)}$ can be written as

$$f_i^{(1)}\to\boldsymbol{\mathcal{A}}_i(\mathbf{V})\cdot\nabla\ln T+\boldsymbol{\mathcal{B}}_i(\mathbf{V})\cdot\nabla\ln n_1+\boldsymbol{\mathcal{C}}_i(\mathbf{V})\cdot\nabla\ln n_2+\mathcal{D}_{i,k\ell}(\mathbf{V})\frac{1}{2}\left(\partial_kU_\ell+\partial_\ell U_k-\frac{2}{d}\delta_{k\ell}\nabla\cdot\mathbf{U}\right)+\mathcal{E}_i(\mathbf{V})\nabla\cdot\mathbf{U}, \tag{A.8}$$

where the quantities $\boldsymbol{\mathcal{A}}_i$, $\boldsymbol{\mathcal{B}}_i$, $\boldsymbol{\mathcal{C}}_i$, $\mathcal{D}_{i,k\ell}$ and $\mathcal{E}_i$ are the solutions of a set of coupled linear integral equations. In this paper we are only interested in the first-order contribution to the mass flux $\mathbf{j}_1^{(1)}$. It is defined as

$$\mathbf{j}_1^{(1)}=m_1\int d\mathbf{v}\,\mathbf{V}\,f_1^{(1)}(\mathbf{V}). \tag{A.9}$$

Using eq. (A.8) into eq. (A.9) and taking into account symmetry considerations, one gets the constitutive form for $\mathbf{j}_1^{(1)}$ given by eq. (7), where

$$D_1^T=-\frac{m_1}{\rho d}\int d\mathbf{v}\mathbf{V}\cdot\boldsymbol{\mathcal{A}}_1(\mathbf{V}) \tag{A.10}$$

is the thermal diffusion coefficient,

$$D_{11}=-\frac{\rho}{m_1n_1d}\int d\mathbf{v}\mathbf{V}\cdot\boldsymbol{\mathcal{B}}_1(\mathbf{V}) \tag{A.11}$$

is the kinetic diffusion coefficient and

$$D_{12}=-\frac{\rho}{m_2n_2d}\int d\mathbf{v}\mathbf{V}\cdot\boldsymbol{\mathcal{C}}_1(\mathbf{V}) \tag{A.12}$$

is the mutual diffusion coefficient. In the above equations $\rho=m_1n_1+m_2n_2$ is the total mass density. According to eqs. (A.10–A.12), only the coefficients $\boldsymbol{\mathcal{A}}_1$, $\boldsymbol{\mathcal{B}}_1$, and $\boldsymbol{\mathcal{C}}_1$ are involved in the evaluation of the mass transport $\mathbf{j}_1^{(1)}$. These quantities are the solutions of the following set of linear integral equations:

$$-\frac{\zeta_1^{(0)}T_1}{2m_1}\frac{\partial^2}{\partial V^2}\boldsymbol{\mathcal{A}}_1+\mathcal{L}_1\boldsymbol{\mathcal{A}}_1+\mathcal{M}_1\boldsymbol{\mathcal{A}}_2=\mathbf{A}_1, \tag{A.13}$$

$$-\frac{\zeta_1^{(0)}T_1}{2m_1}\frac{\partial^2}{\partial V^2}\boldsymbol{\mathcal{B}}_1+\mathcal{L}_1\boldsymbol{\mathcal{B}}_1+\mathcal{M}_1\boldsymbol{\mathcal{B}}_2=\mathbf{B}_1, \tag{A.14}$$

$$-\frac{\zeta_1^{(0)}T_1}{2m_1}\frac{\partial^2}{\partial V^2}\boldsymbol{\mathcal{C}}_1+\mathcal{L}_1\boldsymbol{\mathcal{C}}_1+\mathcal{M}_1\boldsymbol{\mathcal{C}}_2=\mathbf{C}_1. \tag{A.15}$$

Here, we have introduced the linear operators

$$\mathcal{L}_1\boldsymbol{\mathcal{A}}_1=-\left(J_{11}^{(0)}\left[\boldsymbol{\mathcal{A}}_1,f_1^{(0)}\right]+J_{11}^{(0)}\left[f_1^{(0)},\boldsymbol{\mathcal{A}}_1\right]+J_{12}^{(0)}\left[\boldsymbol{\mathcal{A}}_1,f_2^{(0)}\right]\right),$$
$$\mathcal{M}_1\boldsymbol{\mathcal{A}}_2=-J_{12}^{(0)}\left[f_1^{(0)},\boldsymbol{\mathcal{A}}_2\right] \tag{A.16}$$

and the inhomogeneous terms $\mathbf{A}_i$, $\mathbf{B}_i$ and $\mathbf{C}_i$ of the integral equations (A.13–A.15) can be easily obtained for a binary mixture from eqs. (6.17) and (6.18) of ref. [19]. Note that, in contrast to what happens in the undriven case [19], here each one of the quantities $\boldsymbol{\mathcal{A}}_i$, $\boldsymbol{\mathcal{B}}_i$, and $\boldsymbol{\mathcal{C}}_i$ obeys closed integral equations.

For practical purposes, the integral equations (A.13–A.15) must be approximately solved by using a Sonine polynomial expansion. In the lowest Sonine approximation, the quantities $\boldsymbol{\mathcal{A}}_i$, $\boldsymbol{\mathcal{B}}_i$ and $\boldsymbol{\mathcal{C}}_i$ are approximated by

$$\boldsymbol{\mathcal{A}}_1(\mathbf{V})\to-f_{1,M}\mathbf{V}\frac{\rho}{n_1T_1}D_1^T,$$
$$\boldsymbol{\mathcal{A}}_2(\mathbf{V})\to f_{2,M}\mathbf{V}\frac{\rho}{n_2T_2}D_1^T, \tag{A.17}$$

$$\boldsymbol{\mathcal{B}}_1(\mathbf{V}) \to -f_{1,M}\mathbf{V}\frac{m_1^2 n_1}{\rho n_1 T_1}D_{11},$$
$$\boldsymbol{\mathcal{B}}_2(\mathbf{V}) \to f_{2,M}\mathbf{V}\frac{m_2^2 n_2}{\rho n_2 T_2}D_{11}, \tag{A.18}$$
$$\boldsymbol{\mathcal{C}}_1(\mathbf{V}) \to -f_{1,M}\mathbf{V}\frac{m_1 m_2 n_2}{\rho n_1 T_1}D_{12},$$
$$\boldsymbol{\mathcal{C}}_2(\mathbf{V}) \to f_{2,M}\mathbf{V}\frac{m_1 m_2 n_1}{\rho n_2 T_2}D_{12}. \tag{A.19}$$

Upon writing (A.17–A.19) use has been made of the identity $\mathbf{j}_1^{(1)} = -\mathbf{j}_2^{(1)}$. To get the transport coefficients D_1^T, D_{11} and D_{12}, we substitute first $\boldsymbol{\mathcal{A}}_i$, $\boldsymbol{\mathcal{B}}_i$ and $\boldsymbol{\mathcal{C}}_i$ by their Sonine approximations (A.17–A.19), respectively, and then, we multiply the integral equations (A.13–A.15) by $m_1\mathbf{V}$ and integrate over the velocity. After some algebra, one gets the final expressions

$$D_1^T = -\frac{p\rho_1}{\nu_D\rho^2}\left(1-\frac{\rho n_1 T_1}{\rho_1 p}\right)+\frac{\pi^{d/2}}{d\Gamma\left(\frac{d}{2}\right)}\frac{n_1 T}{\rho\nu_D}$$
$$\sum_{j=1}^{2} n_j\mu_{1j}\chi_{1j}^{(0)}\sigma_{1j}^d\gamma_j(1+\alpha_{1j}), \tag{A.20}$$

$$D_{ij} = \frac{\rho}{m_i m_j\nu_D}\frac{\partial}{\partial n_j}(n_i T_i)-\frac{n_i}{m_j\nu_D}\frac{\partial p}{\partial n_j}$$
$$+\frac{\pi^{d/2}}{d\Gamma\left(\frac{d}{2}\right)}\frac{\rho n_i T}{m_j\nu_D}\sum_{\ell=1}^{2}\chi_{i\ell}^{(0)}\,\sigma_{i\ell}^d\,\mu_{\ell i}(1+\alpha_{i\ell})$$
$$\times\left\{\left(\frac{\gamma_i}{m_i}+\frac{\gamma_\ell}{m_\ell}\right)\left[\delta_{j\ell}+\frac{1}{2}\frac{n_\ell}{n_j}\left(n_j\frac{\partial}{\partial n_j}\ln\chi_{i\ell}^{(0)}+I_{i\ell j}\right)\right]\right.$$
$$\left.+\frac{n_\ell\gamma_\ell}{m_\ell}\frac{\partial}{\partial n_j}\ln\gamma_\ell\right\}, \tag{A.21}$$

where

$$\nu_D = \frac{2\pi^{(d-1)/2}}{d\Gamma\left(\frac{d}{2}\right)}\sigma_{12}^{d-1}v_0\chi_{12}^{(0)}(1+\alpha_{12})\left(\frac{\theta_1+\theta_2}{\theta_1\theta_2}\right)^{1/2}$$
$$\times\left(n_2\mu_{21}+n_1\mu_{12}\right). \tag{A.22}$$

The quantities $I_{i\ell j}$ are the origin of the primary difference between the standard Enskog theory and the revised version for elastic collisions. They are zero if $i=\ell$, but otherwise are not zero. In general, they are defined through the relation [20]

$$\sum_{\ell=1}^{2} n_\ell\chi_{i\ell}^{(0)}\sigma_{i\ell}^d\left(n_\ell\partial_{n_j}\ln\chi_{i\ell}^{(0)}+I_{i\ell j}\right)$$
$$=\frac{n_j}{B_2}\left[\frac{1}{T}\left(\frac{\partial\mu_i}{\partial n_j}\right)_{T,n_{k\neq j}}-\frac{1}{n_i}\delta_{ij}-2B_2\chi_{ij}^{(0)}\sigma_{ij}^d\right], \tag{A.23}$$

where

$$B_2 = \frac{\pi^{d/2}}{d\Gamma\left(\frac{d}{2}\right)}, \tag{A.24}$$

and μ_i is the chemical potential of species i.

In the tracer limit ($x_1 \to 0$), the expressions of the (reduced) transport coefficients defined by (10) with $\nu_0 = n_2\sigma_{22}^{d-1}\sqrt{2T_2/m_2}$ [47] become

$$D_{11}^* = \frac{\gamma}{\nu_D^*}, \tag{A.25}$$

$$D_1^{T*} = -\frac{M}{\nu_D^*}\left(p^*-\frac{\gamma}{M}\right)+\frac{(1+\omega)^d}{2\nu_D^*}\frac{M}{1+M}\chi_{12}^{(0)}\phi(1+\alpha_{12}), \tag{A.26}$$

$$D_{12}^* = -\frac{M}{\nu_D^*}\beta+\frac{1}{2\nu_D^*}\frac{\gamma+M}{1+M}\frac{\phi}{T}\left(\frac{\partial\mu_1}{\partial\phi}\right)_{T,n_1}(1+\alpha_{12}), \tag{A.27}$$

where $M = m_1/m_2$, $\omega = \sigma_1/\sigma_2$, $\beta = p^* + \phi\partial_\phi p^*$, p^* is given by eq. (23) and

$$\nu_D^* = \frac{2\pi^{(d-1)/2}}{d\Gamma\left(\frac{d}{2}\right)}\left(\frac{\sigma_{12}}{\sigma_2}\right)^{d-1}\frac{\chi_{12}^{(0)}}{1+M}\sqrt{\frac{M+\gamma}{M}}(1+\alpha_{12}). \tag{A.28}$$

References

1. A. Rosato, K.J. Strandburg, F. Prinz, R.H. Swendsen, Phys. Rev. Lett. **58**, 1038 (1987).
2. J.B. Knight, H.M. Jaeger, S.R. Nagel, Phys. Rev. Lett. **70**, 3728 (1993).
3. J. Duran, J. Rajchenbach, E. Clément, Phys. Rev. Lett. **70**, 2431 (1993).
4. W. Cooken, S. Warr, J.M. Huntley, R.C. Ball, Phys. Rev. E **53**, 2812 (1996).
5. T. Shinbrot, F.J. Muzzio, Phys. Rev. Lett. **81**, 4365 (1998).
6. D.C. Hong, P.V. Quinn, S. Luding, Phys. Rev. Lett. **86**, 3423 (2001).
7. S. Luding, E. Clément, A. Blumen, J. Rajchenbach, J. Duran, Phys. Rev. E **50**, R1762 (1994).
8. M.E. Möbius, B.E. Lauderdale, S.R. Nagel, H.M. Jaeger, Nature **414**, 270 (2001).
9. D. Serero, I. Goldhirsch, S.H. Noskowicz, M.-L. Tan, J. Fluid Mech. **554**, 237 (2006).
10. J.J. Brey, M.J. Ruiz-Montero, F. Moreno, Phys. Rev. Lett. **95**, 098001 (2005); Phys. Rev. E **73**, 031301 (2006).
11. V. Garzó, Europhys. Lett. **75**, 521 (2006).
12. J.T. Jenkins, D. Yoon, Phys. Rev. Lett. **88**, 194301 (2002).
13. B. Arnarson, J.T. Willits, Phys. Fluids **10**, 1324 (1998).
14. B. Arnarson, J.T. Jenkins, Phys. Fluids **16**, 4543 (2004).
15. L. Trujillo, M. Alam, H.J. Herrmann, Europhys. Lett. **64**, 190 (2003); M. Alam, L. Trujillo, H.J. Herrmann, J. Stat. Phys. **124**, 587 (2006).
16. J. Jenkins, F. Mancini, J. Appl. Mech. **54**, 27 (1987).
17. A. Barrat, E. Trizac, Granular Matter **4**, 57 (2002).
18. S.R. Dahl, C.M. Hrenya, V. Garzó, J.W. Dufty, Phys. Rev. E **66**, 041301 (2002).
19. V. Garzó, J.W. Dufty, C.M. Hrenya, Phys. Rev. E **76**, 031303 (2007).
20. V. Garzó, C.M. Hrenya, J.W. Dufty, Phys. Rev. E **76**, 031304 (2007).
21. M. Schröter, S. Ulrich, J. Kreft, S.B. Swift, H.L. Swinney, Phys. Rev. E **74**, 011307 (2006).
22. J.E. Galvin, S.R. Dahl, C.M. Hrenya, J. Fluid Mech. **528**, 207 (2005).

23. A.P.J. Breu, H.M. Ensner, C.A. Kruelle, I. Rehberg, Phys. Rev. Lett. **90**, 014302 (2003).
24. V. Garzó, Phys. Rev. E **78**, 020301(R) (2008).
25. A. Prevost, D.A. Egolf, J.S. Urbach, Phys. Rev. Lett. **89**, 084301 (2002).
26. See, for instance, A. Puglisi, V. Loreto, U.M.B. Marconi, A. Petri, A. Vulpiani, Phys. Rev. Lett. **81**, 3848 (1998); Phys. Rev. E **59**, 5582 (1999); T.P.C. van Noije, M.H. Ernst, E. Trizac, I. Pagonabarraga, Phys. Rev. E **59**, 4326 (1999); R. Cafiero, S. Luding, H.J. Herrmann, Phys. Rev. Lett. **84**, 6014 (2000); S.J. Moon, M.D. Shattuck, J.B. Swift, Phys. Rev. E **64**, 031303 (2001); I. Pagonabarraga, E. Trizac, T.P.C. van Noije, M.H. Ernst, Phys. Rev. E **65**, 011303 (2002).
27. J.M. Kincaid, E.G.D. Cohen, M. López de Haro, J. Chem. Phys. **86**, 963 (1987).
28. S. Chapman, T.G. Cowling, *The Mathematical Theory of Nonuniform Gases* (Cambridge University Press, Cambridge, 1970).
29. See, for instance, J. Lutsko, Phys. Rev. E **63**, 061211 (2001); J. Lutsko, J.J. Brey, J.W. Dufty, Phys. Rev. E **65**, 051304 (2002); X. Yang, C. Huan, D. Candela, R.W. Mair, R.L. Walsworth, Phys. Rev. Lett. **88**, 044301 (2002); C. Huan, X. Yang, D. Candela, R.W. Mair, R.L. Walsworth, Phys. Rev. E **69**, 041302 (2004); J.M. Montanero, V. Garzó, M. Alam, S. Luding, Granular Matter **8**, 103 (2006); G. Lois, A. Lemaître, J.M. Carlson, Phys. Rev. E **76**, 021303 (2007); M.N. Bannerman, T.E. Green, P. Grassia, L. Lue, Phys. Rev. E **79**, 041308 (2009).
30. D.R.M. Williams, F.C. McKintosh, Phys. Rev. E **54**, R9 (1996).
31. C. Henrique, G. Batrouni, D. Bideau, Phys. Rev. E **63**, 011304 (2000).
32. V. Garzó, A. Santos, *Kinetic Theory of Gases in Shear Flows. Nonlinear Transport* (Kluwer, Dordrecht, 2003).
33. See, for instance, J.M. Montanero, V. Garzó, Granular Matter **4**, 17 (2002); R. Pagnani, U.M.B. Marconi, A. Puglisi, Phys. Rev. E **66**, 051304 (2002); P. Krouskop, J. Talbot, Phys. Rev. E **68**, 021304 (2003); H. Wang, G. Jin, Y. Ma, Phys. Rev. E **68**, 031301 (2003).
34. R.D. Wildman, D.J. Parker, Phys. Rev. Lett. **88**, 064301 (2002); K. Feitosa, N. Menon, Phys. Rev. Lett. **88**, 198301 (2002).
35. V. Garzó, J.W. Dufty, Phys. Rev. E **60**, 5706 (1999).
36. A. Santos, J.W. Dufty, Phys. Rev. Lett. **86**, 4823 (2001); Phys. Rev. E **64**, 051305 (2001).
37. T. Boublik, J. Chem. Phys. **53**, 471 (1970); E.W. Grundke, D. Henderson, Mol. Phys. **24**, 269 (1972); L.L. Lee, D. Levesque, Mol. Phys. **26**, 1351 (1973).
38. H.-Q. Wang, N. Menon, Phys. Rev. Lett. **100**, 158001 (2008).
39. V. Garzó, J.W. Dufty, Phys. Rev. E **59**, 5895 (1999).
40. J. Lutsko, Phys. Rev. E **72**, 021306 (2005).
41. V. Garzó, F. Vega Reyes, Phys. Rev. E **79**, 041303 (2009).
42. T.M. Reed, K.E. Gubbins, *Applied Statistical Mechanics* (McGraw-Hill, New York, 1973) Chapter 6.
43. A. Santos, private communication.
44. T. Schautz, R. Brito, C.A. Kruelle, I. Rehberg, Phys. Rev. Lett. **95**, 028001 (2005).
45. R.D. Wildman, J.M. Huntley, D.J. Parker, Phys. Rev. E **63**, 061311 (2001).
46. D.K. Yoon, J.T. Jenkins, Phys. Fluids **18**, 073303 (2006).
47. Note that the form of the effective collision frequency ν_0 chosen here differs slightly from the one considered in ref. [24].